Joint Antenna Selection and Frequency-Domain Scheduling in OFDMA Systems with Imperfect Estimates from Dual Pilot Training Scheme

Salil Kashyap, *Student Member, IEEE*, and Neelesh B. Mehta, *Senior Member, IEEE*

***Abstract*—Transmit antenna selection (AS) has been adopted in contemporary wideband wireless standards such as Long Term Evolution (LTE). We analyze a comprehensive new model for AS that captures several key features about its operation in wideband orthogonal frequency division multiple access (OFDMA) systems. These include the use of channel-aware frequency-domain scheduling (FDS) in conjunction with AS, the hardware constraint that a user must transmit using the same antenna over all its assigned subcarriers, and the scheduling constraint that the subcarriers assigned to a user must be contiguous. The model also captures the novel dual pilot training scheme that is used in LTE, in which a coarse system bandwidth-wide sounding reference signal is used to acquire relatively noisy channel state information (CSI) for AS and FDS, and a dense narrow-band demodulation reference signal is used to acquire accurate CSI for data demodulation. We analyze the symbol error probability when AS is done in conjunction with the channel-unaware, but fair, round-robin scheduling and with channel-aware greedy FDS. Our results quantify how effective joint AS-FDS is in dispersive environments, the interactions between the above features, and the ability of the user to lower SRS power with minimal performance degradation.**

***Index Terms*—Antenna selection, fading channels, OFDMA, scheduling, symbol error probability, diversity techniques, multiple antennas, imperfect channel knowledge.**

I. Introduction

MULTIPLE input multiple output (MIMO) systems improve capacity and provide spatial diversity. However, their use increases the hardware complexity at the transmitter or at the receiver. For example, every antenna element at the transmitter requires a radio frequency (RF) chain consisting of a digital-to-analog converter, an up-converter, and a power amplifier. Antenna selection (AS) is a popular technique that uses fewer RF chains to reduce the hardware complexity [1], [2]. In single transmit AS, the best antenna is selected as a function of instantaneous channel gains. Despite its lower complexity, AS achieves full diversity with perfect and imperfect channel state information (CSI) [3]–[6].

Manuscript received November 8, 2012; revised on February 14, 2013; accepted April 10, 2013. The associate editor coordinating the review of this paper and approving it for publication was A. Sezgin.

The authors are with the Dept. of Electrical Communication Eng., Indian Institute of Science (IISc), Bangalore, India (e-mail: salilkashyap@gmail.com, nbmehta@ece.iisc.ernet.in).

This work was partially supported by a grant from DST, India and EPSRC, UK under the auspices of the India-UK Advanced Technology Center (IU-ATC), and a grant from the Broadcom Foundation, USA.

Digital Object Identifier 10.1109/TWC.2013.060313.121742

Given its advantages, many contemporary standards such as IEEE 802.11n, Long Term Evolution (LTE) [7], and IEEE 802.16m Advanced WiMAX [8] have standardized AS. These wideband standards use orthogonal frequency division multiplexing (OFDM) or orthogonal frequency division multiple access (OFDMA). In wideband frequency-selective channels, AS faces several new challenges. Firstly, different antennas may be optimum for different subcarriers, which can diminish the gains from AS. Secondly, in cellular systems, AS happens in conjunction with frequency-domain scheduling (FDS). Thus, for joint AS-FDS, the BS needs to determine the user and the transmit antenna pair to assign to each subcarrier, and the user transmits with the same antenna over all the subcarriers assigned to it. Thirdly, to limit peak-to-average power ratio (PAPR) and to control signaling overheads, a standard such as LTE constrains the BS to assign only a contiguous group of subcarriers to a user.

Fourthly, in OFDMA systems, training is used to acquire the CSI required not just for data demodulation but also for FDS and AS. Intuitively, determining the best user to assign to a subcarrier and the best antenna it should transmit with requires less accurate channel estimates since the base station (BS) only needs to distinguish among a small number of possibilities. On the other hand, for data demodulation, the channel estimates need to be as accurate as possible. Furthermore, for FDS, the BS needs system bandwidth-wide channel estimates, while for data demodulation it only needs to estimate the channel over the subcarriers assigned to the user. This has led to the adoption of a novel dual pilot training scheme in the LTE uplink. In it, a user transmits a coarse system bandwidth-wide sounding reference signal (SRS) every 2-10 ms to enable the BS to acquire CSI for both AS and FDS. On the other hand, a user transmits a dense demodulation reference signal (DMRS) every time it transmits data – but only on subcarriers that are assigned to it – to enable the BS to get accurate estimates for data demodulation.

Finally, the hardware constraints that motivate AS also affect the OFDMA training procedure. A pilot can be transmitted from only one antenna of a user at a time. Thus, a user alternately sends the SRS from its two transmit antennas, as shown in Fig. 1. The BS estimates the wideband channels of the two transmit antennas to it, and determines and feeds back to the user which subcarriers and which antenna it should use to transmit DMRS and data symbols.

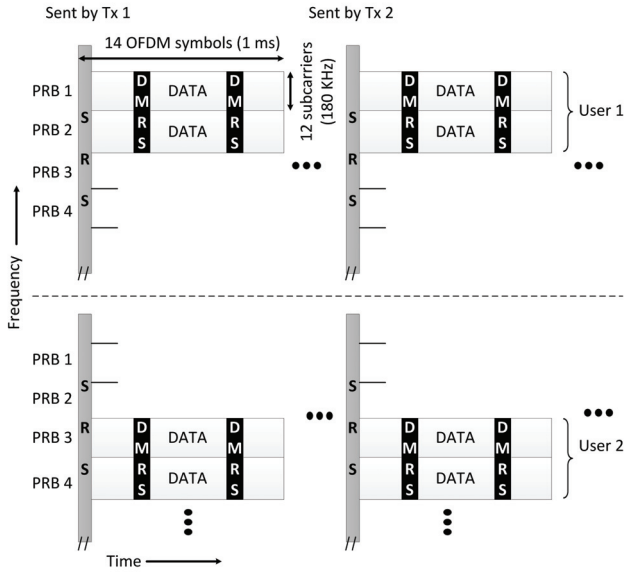

Fig. 1. Illustration of dual pilot training scheme to enable FDS, AS, and coherent data demodulation.

A. Related Literature on AS

We now discuss some key references below.

Flat-fading with Perfect CSI: AS has been extensively investigated in the literature for flat-fading channels. In [9], algorithms for receive AS to maximize capacity are presented. The gap between the capacity of a MIMO system that employs AS and the one that does not is shown in [10], while in [11], the outage probability, symbol error probability (SEP), and capacity for a hybrid selection scheme are analyzed. Joint user scheduling and AS is analyzed in [12]. In [13], the capacity of a multiuser scheduling system for selective transmission or reception is derived. Multiuser diversity gain is derived in terms of the outage probability in [14].

Flat-fading with Imperfect CSI: In [4], the bit error rate (BER) is derived for diversity systems. In [15], the SEP of receive AS with outdated, imperfect CSI for a time-varying channel is analyzed. The pairwise error probability (PEP) of AS in a space-time coded system is derived in [6], and the PEP for both transmit and receive AS is analyzed in [5].

Frequency-selective OFDM Systems with Perfect CSI: In [16], average signal-to-noise-ratio (SNR) gain, outage probability, and BER are analyzed for AS in space-frequency coded OFDM systems. User scheduling schemes without AS for MIMO-OFDM systems that employ orthogonal space-frequency block coding are investigated in [17]. Joint transmitter and receive antenna subset selection for frequency-selective channels is analyzed in [18]. In [19], upper bounds on the PEP of AS in a space-time coded OFDM system are derived. The per-tone AS model, in which different antennas of the same user can be assigned to different subcarriers, is analyzed in [16], [20], [21]. However, no FDS is considered in [20], [21].

Frequency-selective OFDM Systems with Imperfect CSI: In [22], receive AS in a MIMO-OFDM system is analyzed. However, the same pilot, which is always sent with data, is used for both selection and demodulation. Further, no FDS is considered. In [8] and in standards contributions [23], only simulation results are presented for evaluating AS-FDS with dual pilot training.

Thus, while considerable work has been done on AS, its performance analysis in contemporary, wideband OFDMA systems with and without FDS and with imperfect CSI obtained from the dual pilot training scheme remains an open problem, and is the focus of this paper. Borrowing terminology from LTE, we henceforth call the smallest time-frequency resource that can be allocated to a user as a *physical resource block (PRB)*. It consists of F contiguous subcarriers and T OFDMA symbols. For example, in LTE, $F = 12$ and $T = 14$. The smallest data unit consists of one subcarrier and one OFDMA symbol; it is called a *resource element*. Multiple PRBs can be allocated to a user, but they must all be contiguous. A group of C contiguous PRBs is called a *chunk* and the i^{th} chunk consists of the PRBs $(i-1)C+1, \ldots, iC$.

B. Focus and Contributions

To characterize the interactions between AS, FDS, and the scheduling constraints, we analyze the performance of AS in OFDMA systems first with the channel-unaware, but fair, round-robin (RR) scheduler and then with the opportunistic, channel-aware greedy frequency-domain scheduler [24]. Unlike the RR scheduler, the greedy scheduler takes the instantaneous SRS channel gain estimates into account to determine which user to assign to each chunk of PRBs. Altogether, these two schedulers cover a wide range of the throughput vs. fairness trade-off. The performance of other schedulers, e.g., the proportional fair scheduler [25], will lie in between these schedulers.

We first derive a closed-form expression for the SEP of AS with an RR scheduler, in which the BS assigns a chunk of C contiguous PRBs to a user in a pre-determined manner. Only the antenna is selected using the SRS-based channel estimates. The user must use the same antenna to transmit data and DMRS symbols over the entire chunk assigned to it. The analysis takes into account the impact of the imperfect SRS and DMRS-based channel estimates on both AS and data demodulation.

We then analyze AS with FDS, in which both the user and its most appropriate antenna are chosen based on the noisy SRS channel estimates. As before, at most one chunk of C contiguous PRBs is assigned to a user, which then uses the same antenna to transmit data and DMRS symbols. Unlike AS with the RR scheduler, in this case, the SEP of different chunks is different. We, therefore, develop expressions for the SEP chunk by chunk.

We present several numerical that show the effectiveness of AS in dispersive channels even at lower SRS powers, which is a unique advantage of the dual pilot training scheme.

Outline: The paper is organized as follows. The system model is developed in Sec. II. The SEP of AS with the RR scheduler is derived in Sec. III. The SEP of AS with FDS is derived in Sec. IV. Our results and conclusions follow in Sec. V and Sec. VI, respectively.

Notation: We denote matrices and vectors in boldface uppercase and in boldface lowercase, respectively. The conju-

gate, Hermitian transpose, transpose, and determinant operators are denoted by $(.)^*$, $(.)^\dagger$, $(.)^T$, and $\det(.)$, respectively. An $n \times n$ identity matrix is denoted by $\mathbf{I}_n$. The $(i,j)^{\text{th}}$ element of $\mathbf{A}$ is denoted by $(\mathbf{A})_{i,j}$. Further, $\mathbf{A}(\mathbf{r},\mathbf{c})$ denotes the submatrix of $\mathbf{A}$ with $\mathbf{r}$ denoting the vector of row indices and $\mathbf{c}$ denoting the vector of column indices. $\mathbf{A}(:,\mathbf{c})$ denotes the submatrix of $\mathbf{A}$ with all its rows but columns drawn from $\mathbf{c}$. Expectation and variance are denoted by $\mathbf{E}[.]$ and $\mathbf{var}[.]$, respectively. The notation $\mathbf{X} \sim \mathcal{CN}(\mathbf{K})$ means that $\mathbf{X}$ is a circular symmetric complex Gaussian random vector with covariance $\mathbf{K}$. The probability of an event B is denoted by $\Pr(B)$ and the probability density function (pdf) of a random variable (RV) X is denoted by $\mathrm{p}_X(x)$, with the subscript dropped if the RV is obvious from context. Similarly, $\Pr(B|C)$ denotes the conditional probability of B given C, and $\mathrm{p}_{X|Y}(x)$ denotes the conditional pdf of X given Y. The N_{DFT}-point discrete Fourier transform (DFT) matrix is denoted by $\mathbf{\Omega}$.

II. System Model

We consider a multiuser scenario with N users. Each of the users has two transmit antennas and a single transmit RF chain. The receiver has one antenna, as has also been assumed in [4], [15], [26].[1] The i^{th} channel tap of the L-tap baseband channel response arrives with a delay of τ_i, where $0 \le i \le L-1$. Let $\boldsymbol{\tau} = [\tau_0 \ \tau_1 \ \cdots \ \tau_{L-1}]$. The channel gain of the i^{th} tap from the k^{th} antenna of the j^{th} user is denoted by $h_{jk}(i)$. Let $\boldsymbol{h}_{jk} = [h_{jk}(0) \ h_{jk}(1) \ \cdots \ h_{jk}(L-1)]^T$. Further, we assume Rayleigh fading. Therefore, $\boldsymbol{h}_{jk} \sim \mathcal{CN}(\mathbf{\Lambda}_h)$, for $j = 1,\ldots,N$ and $k = 1,2$, and $\mathbf{\Lambda}_h$ is the channel power delay profile and is a diagonal matrix. For all j and k, the channels $\boldsymbol{h}_{jk}$ are independent and identically distributed (i.i.d.). $H_{jk}(n)$ denotes the channel gain of the n^{th} subcarrier of the k^{th} transmit antenna of the j^{th} user.

Comments about Model and Extensions: Our model, which is described in detail below, captures the key features of an AS training model in LTE such as the dual pilot scheme, different quality of estimates for AS, FDS and data demodulation, the use of FDS in conjunction with AS, and the scheduling constraints. Several of these aspects are new relative to what has been analyzed in the AS literature.

However, in order to gain analytical insights, we do make some simplifications. Firstly, we focus on OFDMA and not on single carrier frequency division multiple access (SC-FDMA), which is used in the LTE uplink. Note, however, that OFDMA is being actively considered for the uplink in LTE-Advanced [29]. Secondly, we focus on uncoded transmissions and, thus, evaluate SEP. We do so because the uncoded case is theoretically rich, tractable, and insightful, and has often been analyzed in the AS literature [3], [4], [15], [30]. In general, in the uplink, error control coding along with the precoding techniques, such as DFT spreading [31], are applied across the PRBs. However, these are beyond the scope of this paper.

[1]We note that the analysis gets considerably more involved for the general case with multiple receive antennas even for flat-fading. For example, in [11], [27], numerical techniques are used to invert the characteristic function or the moment generating function. In [28], two special cases involving selecting 2 out of 3 or 4 receive antennas are analyzed, but the resultant SEP expressions are only for binary coherent modulations and are in the form of an infinite series of Gaussian hypergeometric functions.

A. Channel Estimation for AS and FDS Using SRS

A user sends out the wideband SRS alternately from its two transmit antennas to enable the BS to estimate the L-tap channel gains of the user's two transmit antennas. Without loss of generality (w.l.o.g.), the pilot symbols are all set as ones. The frequency-domain signal $\boldsymbol{y}_{jk}^S \in \mathbb{C}^{N_S \times 1}$ received at the BS when the k^{th} antenna of the j^{th} user transmits SRS is

$$\boldsymbol{y}_{jk}^S = \sqrt{E_p^S}\mathbf{\Omega}_{jk}^S \boldsymbol{h}_{jk} + \boldsymbol{w}_{jk}^S, \quad k = 1,2 \text{ and } j = 1,2,\ldots,N, \tag{1}$$

where E_p^S is the average SRS pilot SNR for a subcarrier and $\mathbf{\Omega}_{jk}^S \triangleq \mathbf{\Omega}(\boldsymbol{C}_{jk}^S, \boldsymbol{\tau}) \in \mathbb{C}^{N_S \times L}$ consists of N_S rows of $\mathbf{\Omega}$ that correspond to the set of subcarriers $\boldsymbol{C}_{jk}^S$ on which the N_S SRS pilots are sent out by user j and its antenna k. Its L columns correspond to the tap positions $\boldsymbol{\tau}$. $\boldsymbol{w}_{jk}^S \sim \mathcal{CN}(\boldsymbol{I}_{N_S})$ is complex additive white Gaussian noise (CAWGN).

Given the observables $\boldsymbol{y}_{jk}^S$ from the SRS, the minimum mean square error estimate (MMSE) $\widehat{\boldsymbol{h}}_{jk}^S$ of $\boldsymbol{h}_{jk}$ can be written as [32], $\widehat{\boldsymbol{h}}_{jk}^S = \boldsymbol{m}^\dagger \boldsymbol{y}_{jk}^S$, $k = 1,2$ and $j = 1,2,\ldots,N$, where $\boldsymbol{m}^\dagger = \mathbf{E}\left[\boldsymbol{h}_{jk}\boldsymbol{y}_{jk}^{S\dagger}\right]\left(\mathbf{E}\left[\boldsymbol{y}_{jk}^S\boldsymbol{y}_{jk}^{S\dagger}\right]\right)^{-1} = \sqrt{E_p^S}\mathbf{\Lambda}_h\mathbf{\Omega}_{jk}^{S\dagger}(E_p^S\mathbf{\Omega}_{jk}^S\mathbf{\Lambda}_h\mathbf{\Omega}_{jk}^{S\dagger} + \boldsymbol{I}_{N_S})^{-1}$. The estimate $\widehat{H}_{jk}^S(n)$ of the n^{th} subcarrier gain of the k^{th} transmit antenna of user j is then given by

$$\widehat{H}_{jk}^S(n) = \boldsymbol{\omega}_n \boldsymbol{m}^\dagger \boldsymbol{y}_{jk}^S, \quad k = 1,2 \text{ and } j = 1,2,\ldots,N, \tag{2}$$

where $\boldsymbol{\omega}_n \triangleq \mathbf{\Omega}(n,\boldsymbol{\tau})$.

B. Refined Channel Estimates for Data Demodulation

Let user j and its antenna k be selected. The criterion on the basis of which the users and antenna are selected is specified in Sec. III and Sec. IV. In the chunk of C contiguous PRBs that are assigned to the user, let $\boldsymbol{C}_{jk}^D$ denote the set of N_D subcarriers on which it transmits the DMRS from antenna k.[2] We assume that the duration of the PRB is smaller than the coherence time of the channel, which is justified since a PRB duration is of the order of a millisecond. The frequency-domain signal $\boldsymbol{y}_{jk}^D \in \mathbb{C}^{N_D \times 1}$ received over these N_D subcarriers is

$$\boldsymbol{y}_{jk}^D = \sqrt{E_p^D}\mathbf{\Omega}_{jk}^D \boldsymbol{h}_{jk} + \boldsymbol{w}_{jk}^D, \tag{3}$$

where, w.l.o.g., all the DMRS symbols are set to one, E_p^D is the average DMRS SNR per subcarrier, $\mathbf{\Omega}_{jk}^D \triangleq \mathbf{\Omega}(\boldsymbol{C}_{jk}^D, \boldsymbol{\tau}) \in \mathbb{C}^{N_D \times L}$, and $\boldsymbol{w}_{jk}^D \sim \mathcal{CN}(\boldsymbol{I}_{N_D})$ is CAWGN.

The receiver has access to both the SRS and the DMRS observables from the selected antenna of the best user. Therefore, for accurate coherent data demodulation, it uses both of them to obtain a refined time-domain MMSE estimate $\widetilde{\boldsymbol{h}}_{jk}$ of the L-tap channel. It is given by $\widetilde{\boldsymbol{h}}_{jk} = \boldsymbol{g}^\dagger \left[\boldsymbol{y}_{jk}^{S\dagger} \ \ \boldsymbol{y}_{jk}^{D\dagger}\right]^\dagger$,

[2]Note that in the LTE uplink, the DMRS is sent once in every two subcarriers in the 4^{th} and the 11^{th} OFDM symbols of a PRB. We assume that the channel does not change over the 1 ms duration of a PRB. This is, therefore, equivalent to a single OFDM symbol that is dedicated for DMRS transmission in which all the subcarriers allotted to a user carry pilot symbols.

where, using (1), (3), and the orthogonality principle [32], it can be shown that

$$\boldsymbol{g}^{\dagger} = \begin{bmatrix} \mathbf{E}\left[\boldsymbol{h}_{jk}\boldsymbol{y}_{jk}^{S^{\dagger}}\right] & \mathbf{E}\left[\boldsymbol{h}_{jk}\boldsymbol{y}_{jk}^{D^{\dagger}}\right] \end{bmatrix} \times \begin{bmatrix} \mathbf{E}\left[\boldsymbol{y}_{jk}^{S}\boldsymbol{y}_{jk}^{S^{\dagger}}\right] & \mathbf{E}\left[\boldsymbol{y}_{jk}^{S}\boldsymbol{y}_{jk}^{D^{\dagger}}\right] \\ \mathbf{E}\left[\boldsymbol{y}_{jk}^{D}\boldsymbol{y}_{jk}^{S^{\dagger}}\right] & \mathbf{E}\left[\boldsymbol{y}_{jk}^{D}\boldsymbol{y}_{jk}^{D^{\dagger}}\right] \end{bmatrix}^{-1}. \quad (4)$$

This simplifies to

$$\boldsymbol{g}^{\dagger} = \boldsymbol{\Lambda}_h \begin{bmatrix} \sqrt{E_p^S}\boldsymbol{\Omega}_{jk}^{S^{\dagger}} & \sqrt{E_p^D}\boldsymbol{\Omega}_{jk}^{D^{\dagger}} \end{bmatrix} \begin{bmatrix} \boldsymbol{A}' & \boldsymbol{B}' \\ \boldsymbol{C}' & \boldsymbol{D}' \end{bmatrix}^{-1}, \quad (5)$$

where $\boldsymbol{A}' = E_p^S\boldsymbol{\Omega}_{jk}^{S}\boldsymbol{\Lambda}_h\boldsymbol{\Omega}_{jk}^{S^{\dagger}} + \boldsymbol{I}_{N_S}$, $\boldsymbol{B}' = \boldsymbol{C}'^{\dagger} = \sqrt{E_p^S}\sqrt{E_p^D}\boldsymbol{\Omega}_{jk}^{S}\boldsymbol{\Lambda}_h\boldsymbol{\Omega}_{jk}^{D^{\dagger}}$, and $\boldsymbol{D}' = E_p^D\boldsymbol{\Omega}_{jk}^{D}\boldsymbol{\Lambda}_h\boldsymbol{\Omega}_{jk}^{D^{\dagger}} + \boldsymbol{I}_{N_D}$. Therefore, the refined frequency-domain channel gain estimate $\widetilde{H}_{jk}(n)$ of the n^{th} subcarrier for the selected user j and its antenna k is given by

$$\widetilde{H}_{jk}(n) = \boldsymbol{\omega}_n\widetilde{\boldsymbol{h}}_{jk} = \boldsymbol{\omega}_n\boldsymbol{g}^{\dagger}\begin{bmatrix} \boldsymbol{y}_{jk}^{S^{\dagger}} & \boldsymbol{y}_{jk}^{D^{\dagger}} \end{bmatrix}^{\dagger}. \quad (6)$$

The resource elements in the chunk of PRBs assigned to user j that are not used for DMRS or SRS pilots are used for data transmission. When the user transmits a data symbol X_d on the n^{th} subcarrier, the signal $Y_{jk}(n)$ received on that subcarrier is

$$Y_{jk}(n) = H_{jk}(n)X_d + W_{jk}(n), \quad (7)$$

where $W_{jk}(n) \sim \mathcal{CN}(1)$ is CAWGN. The data symbols are drawn from the MPSK constellation with uniform probability. Let $E_s = \mathbf{E}\left[|X_d|^2\right]$ denote the data SNR per subcarrier.

III. SEP Analysis: AS with RR Scheduler

In the RR scheduler, every chunk of C contiguous PRBs is assigned to a different user in a pre-determined manner without considering the estimated channel gains. However, the antenna is selected based on the estimated SRS channel gains. The selected antenna is used for transmission over all the C contiguous PRBs that are assigned to the user.

Selection Rule: Consider the i^{th} chunk of PRBs. Let user u and its antenna s be selected for it. Let $\hat{\phi}_i = us$, where the notation $\hat{\cdot}$ emphasizes the fact that selection is based on noisy estimates. As mentioned, with the RR scheduler, the choice of u does not depend on the SRS channel gains. The antenna s is selected on the basis of the following rule, which we shall refer to as the *sum rule*. It takes into account the SRS-based channel estimates of all the PRBs assigned to it and ensures that the performance is the same over all of them. Let n_p denote the first subcarrier of the p^{th} PRB. Then, the sum rule is given by

$$s = \arg\max_{l=1,2}\left\{\left|\sum_{p=(i-1)C+1}^{iC}\widehat{H}_{ul}^{S}(n_p)\right|\right\}. \quad (8)$$

Comments About the Sum Rule:

1) For contiguous PRB allocations, the sum rule works as well as the rule that compares the Euclidean norm of the estimates $\left(\sum_{p=(i-1)C+1}^{iC}\left|\widehat{H}_{ul}^{S}(n_p)\right|^2\right)$ even for dispersive channels such as the typical urban (TU) channel [33]. This is because the channel gains of subcarriers within a PRB are highly correlated.
2) The sum rule can be generalized to compare the sums of the subcarrier gain estimates of all the subcarriers in the allocated PRBs instead of just their first subcarriers. Our analysis easily carries over because it still needs to deal with sums of correlated complex Gaussians.
3) The sum rule can also be generalized to the case with multiple receive antennas. For example, with two antennas at the receiver, it gets modified to $s = \arg\max_{l=1,2}\left\{\sum_{r=1}^{2}\left|\sum_{p=(i-1)C+1}^{iC}\widehat{H}_{url}^{S}(n_p)\right|^2\right\}$ where s denotes the index of the selected antenna and $\widehat{H}_{url}^{S}(n_p)$ represents the SRS channel gain estimate for the l^{th} transmit antenna and r^{th} receive antenna over the first subcarrier n_p of the p^{th} PRB of the u^{th} user.

Decoding: Consider the n^{th} subcarrier belonging to the i^{th} chunk of PRBs. The maximum likelihood (ML) decision variable for detecting X_d transmitted on the n^{th} subcarrier is

$$\Upsilon_n = \widetilde{H}_{\hat{\phi}_i}(n)^{\dagger}Y_{\hat{\phi}_i}(n) = \widetilde{H}_{\hat{\phi}_i}(n)^{\dagger}(H_{\hat{\phi}_i}(n)X_d + W_{\hat{\phi}_i}(n)). \quad (9)$$

The SEP of MPSK can be written as [34, Chp. 5]

$$\Pr(\text{Err}|\widetilde{H}_{\hat{\phi}_i}(n)) = \frac{1}{\pi}\int_0^{\frac{(M-1)\pi}{M}}\exp\left(-\frac{|\mu_{\Upsilon_n}|^2\sin^2\left(\frac{\pi}{M}\right)}{\sigma_{\Upsilon_n}^2\sin^2\theta}\right)d\theta, \quad (10)$$

where μ_{Υ_n} and $\sigma_{\Upsilon_n}^2$ are the conditional mean and variance, respectively, of Υ_n given X_d, the SRS-based estimates, and the refined estimate. The following lemma characterizes the conditional mean and variance of Υ_n.

Lemma *1:* The conditional mean and variance of Υ_n are given by

$$\mu_{\Upsilon_n} = \boldsymbol{\Psi}_i(n)\boldsymbol{Q}_i(n)X_d\left|\widetilde{H}_{\hat{\phi}_i}(n)\right|^2, \quad (11)$$

$$\sigma_{\Upsilon_n}^2 = \left|\widetilde{H}_{\hat{\phi}_i}(n)\right|^2\left(1 + E_s\boldsymbol{\omega}_n\boldsymbol{\Lambda}_h\boldsymbol{\omega}_n^{\dagger} - E_s\boldsymbol{\Psi}_i(n)\boldsymbol{\Delta}_i(n)^{-1}\boldsymbol{\Psi}_i(n)^{\dagger}\right), \quad (12)$$

where, for the i^{th} chunk,

$$(\boldsymbol{\Psi}_i(n))_{11} = (\boldsymbol{\Delta}_i(n))_{11} = \boldsymbol{\omega}_n\boldsymbol{g}^{\dagger}\begin{bmatrix}\sqrt{E_p^S}\boldsymbol{\Omega}_{\hat{\phi}_i}^{S} \\ \sqrt{E_p^D}\boldsymbol{\Omega}_{\hat{\phi}_i}^{D}\end{bmatrix}\boldsymbol{\Lambda}_h\boldsymbol{\omega}_n^{\dagger}, \quad (13a)$$

$$(\boldsymbol{\Psi}_i(n))_{12} = \sqrt{E_p^S}\boldsymbol{\omega}_n\boldsymbol{\Lambda}_h\boldsymbol{\Omega}_{\hat{\phi}_i}^{S^{\dagger}}\boldsymbol{m}\boldsymbol{\omega}_s^{\dagger}, \quad (13b)$$

$$(\boldsymbol{\Delta}_i(n))_{12} = (\boldsymbol{\Delta}_i(n))_{21}^{\dagger} = \boldsymbol{\omega}_n\boldsymbol{g}^{\dagger}\begin{bmatrix}E_p^S\boldsymbol{\Omega}_{\hat{\phi}_i}^{S}\boldsymbol{\Lambda}_h\boldsymbol{\Omega}_{\hat{\phi}_i}^{S^{\dagger}} + \mathbf{I}_{N_S} \\ \sqrt{E_p^SE_p^D}\boldsymbol{\Omega}_{\hat{\phi}_i}^{D}\boldsymbol{\Lambda}_h\boldsymbol{\Omega}_{\hat{\phi}_i}^{S^{\dagger}}\end{bmatrix}\boldsymbol{m}\boldsymbol{\omega}_s^{\dagger}, \quad (13c)$$

$$(\boldsymbol{\Delta}_i(n))_{22} = \boldsymbol{\omega}_s\boldsymbol{m}^{\dagger}\left(E_p^S\boldsymbol{\Omega}_{\hat{\phi}_i}^{S}\boldsymbol{\Lambda}_h\boldsymbol{\Omega}_{\hat{\phi}_i}^{S^{\dagger}} + \mathbf{I}_{N_S}\right)\boldsymbol{m}\boldsymbol{\omega}_s^{\dagger}, \quad (13d)$$

$\boldsymbol{\omega}_s = \sum_{p=(i-1)C+1}^{iC}\boldsymbol{\omega}_{n_p}$, and $\boldsymbol{Q}_i(n) = (\boldsymbol{\Delta}_i(n)^{-1})(:,1)$.

Proof: The proof is relegated to Appendix A. ∎

A key point to note from the above lemma is that μ_{Υ_n} and $\sigma_{\Upsilon_n}^2$ are independent of the SRS-based channel estimates given the refined channel estimate $\widetilde{H}_{\hat{\phi}_i}(n)$. The SEP of AS is then given as follows.

Result *1:* The SEP $P_E^{(i)}(n)$ of the n^{th} subcarrier in the i^{th} chunk is given by

$$P_E^{(i)}(n) = \frac{M-1}{M} - \frac{2}{\pi}\left(\sqrt{\frac{L_i\left(\sigma_i^2+\varphi_i^2\right)}{L_i\left(\sigma_i^2+\varphi_i^2\right)+1}} \times \left[\frac{\pi}{2} + \tan^{-1}\left(\sqrt{\frac{L_i\left(\sigma_i^2+\varphi_i^2\right)}{L_i\left(\sigma_i^2+\varphi_i^2\right)+1}}\cot\left(\frac{\pi}{M}\right)\right)\right]\right) + \frac{1}{\pi}\left(\sqrt{\frac{L_i\left(2\sigma_i^2+\varphi_i^2\right)}{L_i\left(2\sigma_i^2+\varphi_i^2\right)+2}} \times \left[\frac{\pi}{2} + \tan^{-1}\left(\sqrt{\frac{L_i\left(2\sigma_i^2+\varphi_i^2\right)}{L_i\left(2\sigma_i^2+\varphi_i^2\right)+2}}\cot\left(\frac{\pi}{M}\right)\right)\right]\right), \tag{14}$$

where $L_i = \frac{|\boldsymbol{\Psi}_i(n)\boldsymbol{Q}_i(n)|^2 E_s \sin^2\left(\frac{\pi}{M}\right)}{1+E_s\left(\boldsymbol{\omega}_n\boldsymbol{\Lambda}_h\boldsymbol{\omega}_n^\dagger - \boldsymbol{\Psi}_i(n)\boldsymbol{\Delta}_i(n)^{-1}\boldsymbol{\Psi}_i(n)^\dagger\right)}$, $\sigma_i^2 = \frac{(\boldsymbol{\Delta}_i(n))_{11}(\boldsymbol{\Delta}_i(n))_{22} - \left|(\boldsymbol{\Delta}_i(n))_{12}\right|^2}{(\boldsymbol{\Delta}_i(n))_{22}}$, and $\varphi_i^2 = \frac{\left|(\boldsymbol{\Delta}_i(n))_{12}\right|^2}{(\boldsymbol{\Delta}_i(n))_{22}}$.

Proof: The proof is relegated to Appendix B. ∎

The expression in (14) brings out the dependence of the SEP on the SRS and DMRS powers and on the dispersion in the channel profile, which determines the correlation between the actual and estimated subcarrier channel gains. The above analysis can also be generalized to cover M-QAM.

IV. SEP Analysis: AS With FDS

We now analyze the SEP when both AS and FDS are done on the basis of the noisy SRS channel estimates. As before, C contiguous PRBs are assigned to a user. The user must use the same antenna to transmit the DMRS and data over all the PRBs allotted to it. Once a user is assigned a chunk of C PRBs, it is not considered for subsequent allocations.[3] Let $\mathcal{U} = \{1, 2, \ldots, N\}$ denote the set of users and let $\mathcal{P}$ be the set of PRBs. Let $\hat{\phi}_i$ denote the user and its antenna that get assigned the i^{th} chunk of PRBs. Now, in addition to the antenna, the user is also selected on the basis of the SRS channel estimates. The first chunk of C contiguous PRBs are assigned as per the sum rule as follows:

$$\hat{\phi}_1 = \arg\max_{j\in\mathcal{U},k=1,2}\left\{\left|\sum_{p=1}^{C}\widehat{H}_{jk}^S(n_p)\right|\right\}. \tag{15}$$

Let $\hat{\phi}_1 = u_1 s_1$. The second chunk of PRBs is assigned to the most appropriate user from the set $\mathcal{U}\setminus\{u_1\}$. Specifically,

$$\hat{\phi}_2 = \arg\max_{j\in\mathcal{U}\setminus\{u_1\},k=1,2}\left\{\left|\sum_{p=C+1}^{2C}\widehat{H}_{jk}^S(n_p)\right|\right\}. \tag{16}$$

The process is repeated until all the PRBs get allocated or there are no more users left to assign.

[3]The scenario where the number of chunks assigned to a user is also determined on the basis of the SRS channel estimates is beyond the scope of this paper.

A. SEP Analysis of First Chunk of PRBs

Unlike Sec. III, here the SEP of different chunks is different. We, therefore, analyze the SEP chunk by chunk. Consider a subcarrier n in the first chunk of PRBs. The ML decision variable for detecting the data symbol X_d transmitted by $\hat{\phi}_1$ on the n^{th} subcarrier is $\Upsilon_n = \widetilde{H}_{\hat{\phi}_1}(n)^\dagger Y_{\hat{\phi}_1}(n) = \widetilde{H}_{\hat{\phi}_1}(n)^\dagger(H_{\hat{\phi}_1}(n)X_d + W_{\hat{\phi}_1}(n))$. The conditional mean and variance of Υ_n are given in Lemma 1. The SEP for the first chunk of PRBs is then as follows.

Result *2:* The SEP $P_E^{(1)}(n)$ of the n^{th} subcarrier in the first chunk of PRBs is given by

$$P_E^{(1)}(n) = \frac{2N}{\pi}\int_0^{\frac{(M-1)\pi}{M}}\left(\frac{L_1\sigma_1^2}{\sin^2\theta}+1\right)^{-1} \times B\left(\frac{\varphi_1^2}{\sigma_1^2}+1-\frac{\varphi_1^2}{\sigma_1^2}\left(\frac{L_1\sigma_1^2}{\sin^2\theta}+1\right)^{-1}, 2N\right)d\theta, \tag{17}$$

where L_1, σ_1^2, and φ_1^2 are as defined in Result 1, and $B(\cdot,\cdot)$ is the Beta function [35, (3.312.1)].

Proof: The proof is relegated to Appendix C. ∎

The above SEP expression is in the form of a single integral in θ and is evaluated numerically. Using the inequality $\sin^2\theta \leq 1$, a closed-form SEP upper bound can be obtained as follows.

Corollary *1:* The SEP $P_E^{(1)}(n)$ of the n^{th} subcarrier belonging to the first chunk of PRBs is upper bounded as

$$P_E^{(1)}(n) \leq \frac{2N(M-1)}{M\left(L_1\sigma_1^2+1\right)}B\left(\frac{\varphi_1^2}{\sigma_1^2}+1-\frac{\varphi_1^2}{\sigma_1^2(L_1\sigma_1^2+1)}, 2N\right). \tag{18}$$

B. SEP Analysis of Second Chunk of PRBs

Recall that $\hat{\phi}_2$ denotes the user and its antenna that are selected for the second chunk of PRBs. Consider a subcarrier n in the second chunk of PRBs. The ML decision variable for detecting the data symbol X_d transmitted over the n^{th} subcarrier is $\Upsilon_n = \widetilde{H}_{\hat{\phi}_2}(n)^\dagger Y_{\hat{\phi}_2}(n) = \widetilde{H}_{\hat{\phi}_2}(n)^\dagger(H_{\hat{\phi}_2}(n)X_d + W_{\hat{\phi}_2}(n))$. The conditional mean and variance of Υ_n can again be determined using Lemma 1. The SEP for the second chunk of PRBs is then as follows.

Result *3:* The SEP $P_E^{(2)}(n)$ of the n^{th} subcarrier belonging to the second chunk of PRBs is given by

$$P_E^{(2)}(n) \approx \frac{2N(N-1)}{\pi}\int_0^{\frac{(M-1)\pi}{M}}\left(\frac{L_2\sigma_2^2}{\sin^2\theta}+1\right)^{-1} \times \left[B\left(\frac{\varphi_2^2}{\sigma_2^2}+1-\frac{\varphi_2^2}{\sigma_2^2}\left(\frac{L_2\sigma_2^2}{\sin^2\theta}+1\right)^{-1}, 2N-2\right) - B\left(\frac{\varphi_2^2}{\sigma_2^2}+1-\frac{\varphi_2^2}{\sigma_2^2}\left(\frac{L_2\sigma_2^2}{\sin^2\theta}+1\right)^{-1}, 2N\right)\right]d\theta, \tag{19}$$

where L_2, σ_2^2, and φ_2^2 are as defined in Result 1.

Proof: The proof is given in Appendix D. ∎

The above SEP expression is again in the form of a single integral in θ, and can be written in an integral-free form along the lines of Corollary 1 by replacing $\sin^2\theta$ by 1. The expression is not shown here to conserve space.

General Case of i^{th} Chunk of PRBs: For the i^{th} chunk of PRBs, for $i \geq 3$, the integrand in the SEP formula turns out to be a linear combination of Beta functions of the form

$$\sum_{l=0}^{i-1}(-1)^{l+i-1}\binom{i-1}{l}\left(\frac{L_i\sigma_i^2}{\sin^2\theta}+1\right)^{-1} \times B\left(\frac{\varphi_i^2}{\sigma_i^2}+1-\frac{\varphi_i^2}{\sigma_i^2}\left(\frac{L_i\sigma_i^2}{\sin^2\theta}+1\right)^{-1}, 2(N-l)\right).$$

C. General Lower Bound on the SEP of AS with FDS

We state below a general lower bound result about the SEP that holds for the i^{th} chunk, for all $i \geq 2$. The advantage of this result is its analytical simplicity and its generality.

Result *4:* The SEP of the n^{th} subcarrier in the i^{th} chunk of PRBs, for all $i \geq 2$, is lower bounded by

$$P_E^{(i)}(n) \geq \frac{2(N-i+1)}{\pi}\int_0^{\frac{(M-1)\pi}{M}}\left(\frac{L_1\sigma_1^2}{\sin^2\theta}+1\right)^{-1} \times B\left(\frac{\varphi_1^2}{\sigma_1^2}+1-\frac{\varphi_1^2}{\sigma_1^2}\left(\frac{L_1\sigma_1^2}{\sin^2\theta}+1\right)^{-1}, 2(N-i+1)\right)d\theta, \tag{20}$$

where L_1, σ_1^2, and φ_1^2 are as defined in Result 1.

Proof: The proof is given in Appendix E. ∎

V. Numerical Results

We now numerically study the performance of AS with the schedulers using Monte Carlo simulations that use 10^5 samples, and verify our analysis. To understand the effect of frequency-selectivity, we consider two popular channel profiles, namely, TU and rural area (RA) [33]. The TU channel is quite dispersive, as its maximum delay spread is 2.14 μs and its RMS delay spread is 0.50 μs. On the other hand, the RA channel has a maximum delay spread of only 0.53 μs and an RMS delay spread of only 0.10 μs. For all the simulations, the system bandwidth (BW) and the SRS BW are 5 MHz, the SRS pilots are embedded in one out of every 6 subcarriers, the DMRS symbols are embedded in every subcarrier of the PRBs allocated to the user, the total number of subcarriers is 300, and the DFT size is 512. We allocate $C = 2$ contiguous PRBs to every user. Each PRB consists of 12 subcarriers.

A. AS with RR scheduler

Figure 2 plots the SEP for QPSK as a function of the subcarrier data SNR for the TU channel when $E_p^S = E_p^D = E_s$. The analytical curves match very well with the simulation curves. Also plotted are the curves for ideal single antenna transmission with perfect CSI and ideal AS, in which perfect CSI is available for both selection and data demodulation and different transmit antennas may be used for different PRBs. At an SEP of 10^{-2}, for the sum rule with imperfect CSI, we see that estimation errors induce a marginal loss in SNR of 0.35 dB relative to the sum rule with perfect CSI. The gap between the SEPs of ideal AS and the sum rule with perfect CSI is due to the highly dispersive nature of the TU channel. Even with imperfect CSI, AS outperforms ideal single antenna transmission, with the slopes of the two curves being different as expected. We also see that the received signal power-based selection rule of [22] gives very limited gains for the TU channel. This is because it is better suited for a scenario where the entire bandwidth is allocated to a single user.

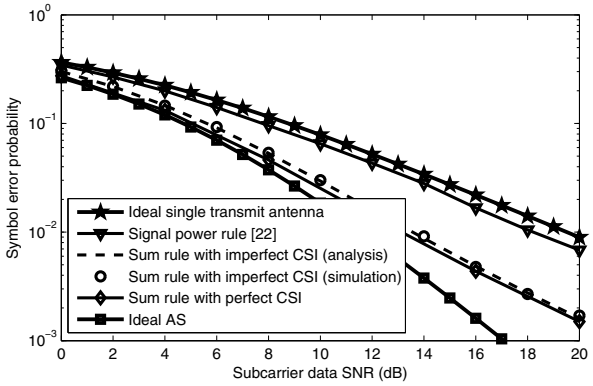

Fig. 2. AS with RR scheduler, TU channel: SEP vs. subcarrier data SNR ($E_p^S = E_p^D = E_s$ and QPSK).

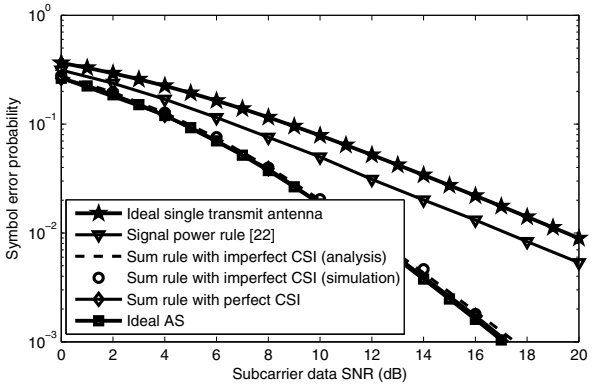

Fig. 3. AS with RR scheduler, RA channel: SEP vs. subcarrier data SNR ($E_p^S = E_p^D = E_s$ and QPSK).

Figure 3 plots the same for the RA channel. Now, the SEP of AS with perfect CSI is very close to ideal AS because the RA channel is less dispersive. As before, AS with imperfect CSI outperforms ideal single antenna transmission. The received signal power-based selection rule fares poorly even here.

Figures 4 and 5 investigate the effect of the SRS power E_p^S on the SEP of 8PSK for the TU and RA channels, respectively. The SEPs for three different SRS SNRs are shown in both the figures. We see that when E_p^S is 5 dB lower than E_s, the loss in SNR at an SEP of 10^{-2} is only 0.25 dB and 0.15 dB for the TU and RA channels, respectively, relative to the case when $E_p^S = E_s$. When E_p^S is 10 dB lower than E_s, the corresponding losses in SNR increase marginally to 0.6 dB and 0.35 dB. The performance, thus, does not degrade much even when the SRS pilot powers are lowered, which is a unique advantage of the dual pilot training scheme.

Figure 6 plots throughput as a function of the subcarrier data SNR for the TU channel. The throughput is defined as the fraction of bits per symbol that reach the destination correctly. This is done for QPSK and 8PSK, and for $C = 2$ and $C = 3$. The analytical results match well with the simulation results.

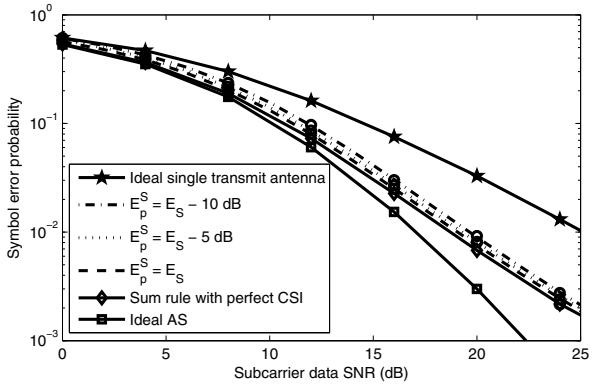

Fig. 4. AS with RR scheduler, TU channel: Effect of SRS power on SEP (8PSK and $E_p^D = E_s$). Simulation results are shown using the marker 'o'.

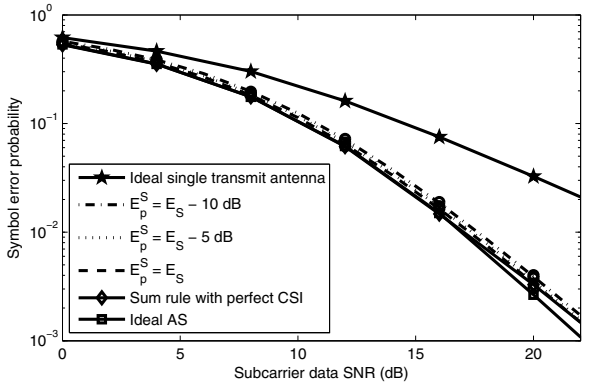

Fig. 5. AS with RR scheduler, RA channel: Effect of SRS power on SEP (8PSK and $E_p^D = E_s$). Simulation results are shown using the marker 'o'.

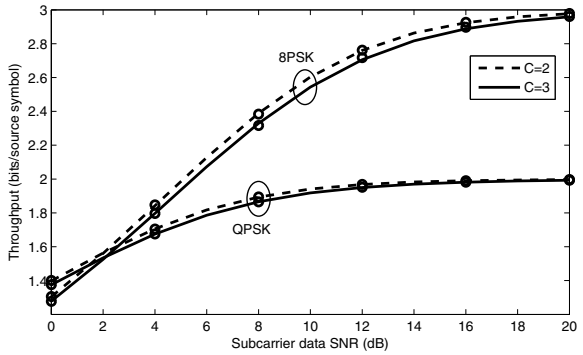

Fig. 6. Throughput of AS as a function of subcarrier data SNR ($E_p^S = E_p^D = E_s$, TU channel, and RR scheduler). Simulation results are shown using the marker 'o'.

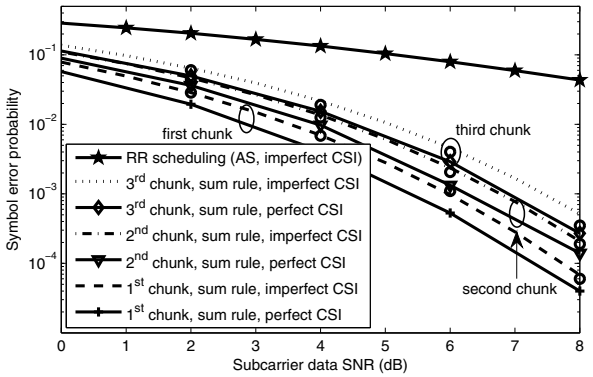

Fig. 7. AS with FDS, RA channel: SEP vs. subcarrier data SNR ($E_p^S = E_p^D = E_s$, QPSK, and $N = 15$ users). Simulation results are shown using the marker 'o'.

We see that $C = 2$ achieves a marginally higher throughput than $C = 3$ because the same antenna is used for transmitting over all the PRBs in a chunk. The trends are similar for the RA channel, except that the curves for $C = 2$ and $C = 3$ are indistinguishable. The trends are also similar for the greedy scheduler; the results are not plotted to conserve space.

B. AS with FDS

Figure 7 plots the SEP of the sum rule for QPSK as a function of the subcarrier data SNR for a subcarrier from the first, second, and third chunks. This is done for the RA channel with $E_p^S = E_p^D = E_s$. The analytical curves match well with the simulation curves, which validates the analysis for AS with FDS. The analysis and simulation results differ marginally by 0.1 dB and 0.2 dB for the second and third chunks, respectively, because of the correlation approximation used in (42) in Appendix D. Also shown are the corresponding SEP curves for the sum rule with: (i) perfect CSI and (ii) RR scheduler. At an SEP of 10^{-3}, imperfect CSI induces a loss in SNR of 0.5 dB for all the chunks. The SEP of AS with FDS degrades for chunks that are allocated later, but is considerably better than that with the RR scheduler.

Figure 8 plots the corresponding curves for the more dispersive TU channel. To avoid clutter, the results for the second chunk are not shown. As in Figure 7, a slight mismatch of 1 dB now arises between the analytical and the simulation curves for the SEP of subcarriers in the third chunk. Now, at an SEP of 10^{-3}, the loss in SNR for a subcarrier in the third chunk is 0.7 dB relative to the first chunk. This is marginally lower than that for the RA channel. Interestingly, from Figures 7 and 8, we see that the gains achieved by AS with FDS over AS with the RR scheduler are more for a more frequency-selective channel. For example, at an SEP of 0.1, while the gain in the case of the RA channel is 4 dB, it is 5.4 dB for the TU channel.

Figure 9 plots the lower and upper bounds (obtained by replacing $\sin^2\theta$ with unity in (19)), and the SEP of the second chunk for the TU channel. The results for the other chunks are not shown to avoid clutter. Notice again the small mismatch of 0.5 dB between the analysis and the simulation results, which is due to the correlated approximation used in Appendix D. The gap reduces to 0.1 dB for the RA channel, the results for which are not plotted to conserve space. The upper bound is within 1 dB of the exact SEP for both channels.

Figure 10 shows the effect of lowering the SRS pilot power on the SEP of the first chunk for AS with FDS for 8PSK. As before, there is only a marginal degradation in the SEP. Joint AS-FDS still outperforms AS with RR scheduler and is quite close to the perfect CSI case as well. A similar behavior is also observed for the RA channel and for other chunks.

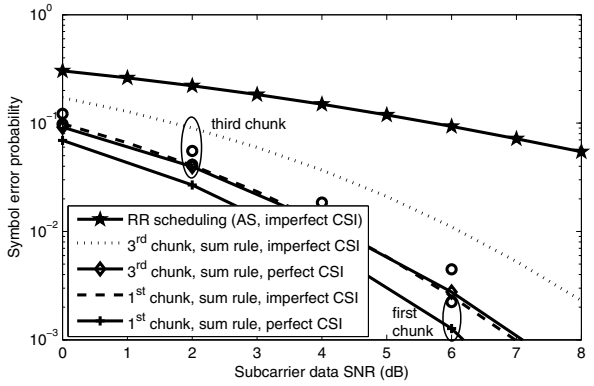

Fig. 8. AS with FDS, TU channel: SEP vs. subcarrier data SNR ($E_p^S = E_p^D = E_s$, QPSK, and $N = 15$ users). Simulation results are shown using the marker '$\circ$'.

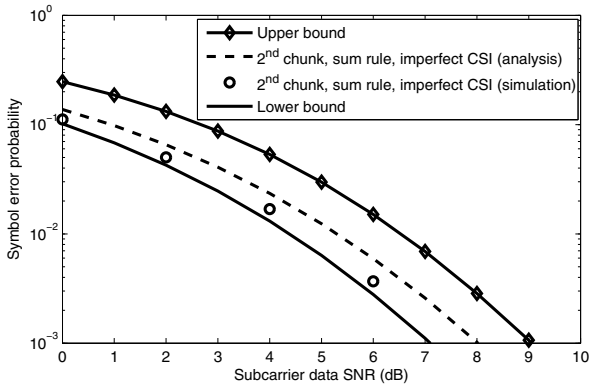

Fig. 9. AS with FDS, TU channel: Lower and upper bounds for the SEP of the 2^{nd} chunk of PRBs ($E_p^S = E_p^D = E_s$, QPSK, and $N = 15$ users).

VI. Conclusions

We analyzed a model for AS that captures several essential features about its implementation in a contemporary, wideband OFDMA cellular system. These include the use of AS in conjunction with FDS, scheduling constraints, and a dual pilot training scheme that provides channel estimates of different accuracies for AS, FDS, and data demodulation. Our SEP analysis accounted for the correlation of the SRS and the DMRS-based estimates across subcarriers and the impact of their noisy nature on user assignment, AS, and data demodulation.

We saw that AS with the sum rule delivers gains even in dispersive channels, and that the contiguous allocation scheduling constraint is, in fact, beneficial for AS. The sum rule outperforms the received signal power rule. The dual pilot training scheme, by its very design, enables the user to transmit the SRS at lower powers compared to DMRS and data powers.

Appendix

A. Brief Proof of Lemma 1

To conserve space, we highlight the main steps below.

Evaluating μ_{Υ_n}: The conditional mean of the decision variable in (9) is given by $\mu_{\Upsilon_n} = \mathbf{E}\left[\Upsilon_n \middle| \widetilde{H}_{\hat{\phi}_i}(n), \widehat{H}^S_{\hat{\phi}_i}(n_{(i-1)C+1}), \cdots, \widehat{H}^S_{\hat{\phi}_i}(n_{iC}), X_d\right]$. The sum rule selects on the basis of $\sum_{p=(i-1)C+1}^{iC} \widehat{H}^S_{\hat{\phi}_i}(n_p)$, and the noise $W_{\hat{\phi}_i}(n)$ is independent of the channel estimates $\widetilde{H}_{\hat{\phi}_i}(n)$, $\widehat{H}^S_{\hat{\phi}_i}(n_{(i-1)C+1})$, $\cdots$, $\widehat{H}^S_{\hat{\phi}_i}(n_{iC})$, and X_d. Hence, μ_{Υ_n} simplifies to

$$\mu_{\Upsilon_n} = \widetilde{H}_{\hat{\phi}_i}(n)^\dagger X_d \mathbf{E}\left[r \middle| \boldsymbol{z}\right] = \widetilde{H}_{\hat{\phi}_i}(n)^\dagger X_d \boldsymbol{\Psi}_i(n) \boldsymbol{\Delta}_i(n)^{-1} \boldsymbol{z}, \tag{21}$$

where $r \triangleq H_{\hat{\phi}_i}(n)$, $\boldsymbol{z} \triangleq \left[\widetilde{H}_{\hat{\phi}_i}(n) \ \sum_{p=(i-1)C+1}^{iC} \widehat{H}^S_{\hat{\phi}_i}(n_p)\right]^T$, $\boldsymbol{\Psi}_i(n)$ is the cross-covariance of r and $\boldsymbol{z}$, and $\boldsymbol{\Delta}_i(n)$ is the covariance of $\boldsymbol{z}$. Here, (21) follows from standard results on conditional Gaussians [32]. The cross-covariance is given by $\boldsymbol{\Psi}_i(n) = \left[\mathbf{E}\left[H_{\hat{\phi}_i}(n)\widetilde{H}_{\hat{\phi}_i}(n)^\dagger\right] \mathbf{E}\left[H_{\hat{\phi}_i}(n) \sum_{p=(i-1)C+1}^{iC} \widehat{H}^S_{\hat{\phi}_i}(n_p)^\dagger\right]\right]$.

Recall that $H_{\hat{\phi}_i}(n) = \boldsymbol{\omega}_n \boldsymbol{h}_{\hat{\phi}_i}$. Furthermore, $\boldsymbol{h}_{\hat{\phi}_i}$ is independent of the noises $\boldsymbol{w}^S_{\hat{\phi}_i}$ and $\boldsymbol{w}^D_{\hat{\phi}_i}$, and $\mathbf{E}\left[\boldsymbol{h}_{\hat{\phi}_i}\boldsymbol{h}^\dagger_{\hat{\phi}_i}\right] = \boldsymbol{\Lambda}_h$. Using these observations along with (5) and (6), it can be shown that $(\boldsymbol{\Psi}_i(n))_{11} = \mathbf{E}\left[H_{\hat{\phi}_i}(n)\ \widetilde{H}_{\hat{\phi}_i}(n)^\dagger\right] = \boldsymbol{\omega}_n \boldsymbol{g}^\dagger \begin{bmatrix} \sqrt{E_p^S}\boldsymbol{\Omega}^S_{\hat{\phi}_i} \\ \sqrt{E_p^D}\boldsymbol{\Omega}^D_{\hat{\phi}_i} \end{bmatrix} \boldsymbol{\Lambda}_h \boldsymbol{\omega}_n^\dagger$. Similarly, $(\boldsymbol{\Psi}_i(n))_{12} = \mathbf{E}\left[H_{\hat{\phi}_i}(n)\ \sum_{p=(i-1)C+1}^{iC} \widehat{H}^S_{\hat{\phi}_i}(n_p)^\dagger\right] = \mathbf{E}\left[\boldsymbol{\omega}_n \boldsymbol{h}_{\hat{\phi}_i}\left(\sqrt{E_p^S}\boldsymbol{\Omega}^S_{\hat{\phi}_i}\boldsymbol{h}_{\hat{\phi}_i} + \boldsymbol{w}^S_{\hat{\phi}_i}\right)^\dagger \boldsymbol{m} \sum_{p=(i-1)C+1}^{iC} \boldsymbol{\omega}_{n_p}^\dagger\right] = \sqrt{E_p^S}\boldsymbol{\omega}_n \boldsymbol{\Lambda}_h \boldsymbol{\Omega}^{S^\dagger}_{\hat{\phi}_i} \boldsymbol{m} \sum_{p=(i-1)C+1}^{iC} \boldsymbol{\omega}_{n_p}^\dagger$.

Next, we evaluate the covariance $\boldsymbol{\Delta}_i(n)$ of $\boldsymbol{z}$. Its four elements are evaluated separately below. From (6), we have

$$\begin{aligned}(\boldsymbol{\Delta}_i(n))_{11} &= \mathbf{E}\left[\left|\widetilde{H}_{\hat{\phi}_i}(n)\right|^2\right], \\ &= \boldsymbol{\omega}_n \boldsymbol{g}^\dagger \begin{bmatrix} \mathbf{E}\left[\boldsymbol{y}^S_{\hat{\phi}_i}\boldsymbol{y}^{S^\dagger}_{\hat{\phi}_i}\right] & \mathbf{E}\left[\boldsymbol{y}^S_{\hat{\phi}_i}\boldsymbol{y}^{D^\dagger}_{\hat{\phi}_i}\right] \\ \mathbf{E}\left[\boldsymbol{y}^D_{\hat{\phi}_i}\boldsymbol{y}^{S^\dagger}_{\hat{\phi}_i}\right] & \mathbf{E}\left[\boldsymbol{y}^D_{\hat{\phi}_i}\boldsymbol{y}^{D^\dagger}_{\hat{\phi}_i}\right] \end{bmatrix} \boldsymbol{g}\boldsymbol{\omega}_n^\dagger.\end{aligned} \tag{22}$$

Using (5), we can show that (22) simplifies to (13a). Its element $(\boldsymbol{\Delta}_i(n))_{12}$ is given by

$$(\boldsymbol{\Delta}_i(n))_{12} = \mathbf{E}\left[\widetilde{H}_{\hat{\phi}_i}(n) \sum_{p=(i-1)C+1}^{iC} \widehat{H}^S_{\hat{\phi}_i}(n_p)^\dagger\right],$$

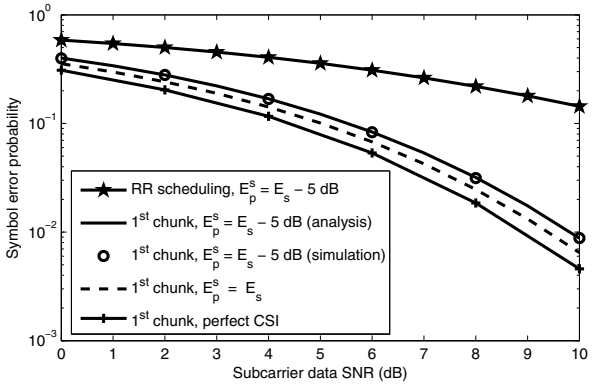

Fig. 10. AS with FDS, TU channel: Effect of lowering the SRS power on the SEP of the 1st chunk (8PSK, $E_p^D = E_s$, and $N = 15$ users).

$$= \left[\boldsymbol{\omega}_n \boldsymbol{g}^\dagger \begin{bmatrix} \mathbf{E}\left[\boldsymbol{y}^S_{\hat{\phi}_i} \boldsymbol{y}^{S^\dagger}_{\hat{\phi}_i}\right] \\ \mathbf{E}\left[\boldsymbol{y}^D_{\hat{\phi}_i} \boldsymbol{y}^{S^\dagger}_{\hat{\phi}_i}\right] \end{bmatrix} \boldsymbol{m} \sum_{p=(i-1)C+1}^{iC} \boldsymbol{\omega}^\dagger_{n_p}\right], \tag{23}$$

where (23) follows from (2) and (6). Using (1) and (3), it can be shown that (23) simplifies to (13c). Similarly, expressions for $(\boldsymbol{\Delta}_i(n))_{21}$ and $(\boldsymbol{\Delta}_i(n))_{22}$ can be derived.

To evaluate μ_{Υ_n} in (21), we need $\boldsymbol{\Psi}_i(n)\left(\boldsymbol{\Delta}_i(n)\right)^{-1}$, which is a 1×2 matrix. Its first element $K_1(n)$, in terms of the first column $\boldsymbol{Q}_i(n)$ of $(\boldsymbol{\Delta}_i(n))^{-1}$, is simply given as $K_1(n) = \boldsymbol{\Psi}_i(n)\left(\boldsymbol{\Delta}_i(n)^{-1}\right)(:,1) = \boldsymbol{\Psi}_i(n)\boldsymbol{Q}_i(n)$. After careful manipulation, it can be shown that its second element is $K_2(n) = \boldsymbol{\Psi}_i(n)\left(\boldsymbol{\Delta}_i(n)^{-1}\right)(:,2) = 0$. Substituting this in (21) yields the desired expression for μ_{Υ_n} in (11).

Evaluating $\sigma^2_{\Upsilon_n}$*:* From (9) and the fact that $\mathbf{E}\left[|X_d|^2\right] = E_s$ and $\mathbf{E}\left[\left|W_{\hat{\phi}_i}(n)\right|^2\right] = 1$, the conditional variance $\sigma^2_{\Upsilon_n}$ is

$$\sigma^2_{\Upsilon_n} = \left|\widetilde{H}_{\hat{\phi}_i}(n)\right|^2 \left(1 + E_s \ \mathbf{var}\left[r|\boldsymbol{z}\right]\right). \tag{24}$$

Again using standard results on conditional Gaussians [32], we can show that $\mathbf{var}\left[r|\boldsymbol{z}\right] = \mathbf{var}\left[r\right] - \boldsymbol{\Psi}_i(n)\boldsymbol{\Delta}_i(n)^{-1}\boldsymbol{\Psi}_i(n)^\dagger = \boldsymbol{\omega}_n\boldsymbol{\Lambda}_h\boldsymbol{\omega}_n^\dagger - \boldsymbol{\Psi}_i(n)\boldsymbol{\Delta}_i(n)^{-1}\boldsymbol{\Psi}_i(n)^\dagger$. Substituting this in (24) yields (12).

B. Proof of Result 1

Let $O^{(i)}_{us} \triangleq \sum_{p=(i-1)C+1}^{iC} \widehat{H}^S_{us}(n_p)$. By symmetry, the probability $P_E^{(i)}(n)$ that a symbol transmitted on the n^{th} subcarrier of the i^{th} chunk of PRBs is in error (Err) is

$$P_E^{(i)}(n) = 2\Pr(\text{Err}, \hat{\phi}_i = u1) = 2\Pr(\text{Err}, |O^{(i)}_{u2}| < |O^{(i)}_{u1}|). \tag{25}$$

Conditioning on the refined estimate, we get[4]

$$P_E^{(i)}(n) = 2\int_0^\infty \Pr(\text{Err}\big||\widetilde{H}_{u1}(n)| = x, |O^{(i)}_{u2}| < |O^{(i)}_{u1}|) \times \mathrm{p}(|\widetilde{H}_{u1}(n)| = x, |O^{(i)}_{u2}| < |O^{(i)}_{u1}|)\, dx. \tag{26}$$

From Lemma 1, given the refined estimate $\widetilde{H}_{u1}(n)$, the decision variable is independent of the SRS-based channel estimates. Hence, the above equation simplifies to

$$P_E^{(i)}(n) = 2\int_0^\infty \Pr(\text{Err}\big||\widetilde{H}_{u1}(n)| = x) \times \mathrm{p}(|\widetilde{H}_{u1}(n)| = x, |O^{(i)}_{u2}| < |O^{(i)}_{u1}|)\, dx. \tag{27}$$

From (10), we know that first term in the integrand above is

$$\Pr(\text{Err}\big||\widetilde{H}_{u1}(n)| = x) = \frac{1}{\pi}\int_0^{\frac{(M-1)\pi}{M}} \exp\left(-\frac{L_i x^2}{\sin^2\theta}\right) d\theta, \tag{28}$$

where $L_i = \frac{|\boldsymbol{\Psi}_i(n)\boldsymbol{Q}_i(n)|^2 E_s \sin^2\left(\frac{\pi}{M}\right)}{1+E_s\left(\boldsymbol{\omega}_n\boldsymbol{\Lambda}_h\boldsymbol{\omega}_n^\dagger - \boldsymbol{\Psi}_i(n)\boldsymbol{\Delta}_i(n)^{-1}\boldsymbol{\Psi}_i(n)^\dagger\right)}$ follows from (11) and (12).

We now evaluate the second term $\mathrm{p}(|\widetilde{H}_{u1}(n)| = x, |O^{(i)}_{u2}| < |O^{(i)}_{u1}|)$ in the integrand in (27). Conditioning on $O^{(i)}_{u1}$, we have $\mathrm{p}(|\widetilde{H}_{u1}(n)| = x, |O^{(i)}_{u2}| < |O^{(i)}_{u1}|) = \mathbf{E}\left[\mathrm{p}(|\widetilde{H}_{u1}(n)| = x, |O^{(i)}_{u2}| < |O^{(i)}_{u1}|)\Big|O^{(i)}_{u1}\right]$. Since $O^{(i)}_{u2}$ is independent of $\widetilde{H}_{u1}(n)$, we get

$$\mathrm{p}(|\widetilde{H}_{u1}(n)| = x, |O^{(i)}_{u2}| < |O^{(i)}_{u1}|) = \mathbf{E}\left[\mathrm{p}_{\left|\widetilde{H}_{u1}(n)\right|\left|O^{(i)}_{u1}\right.}(x)\Pr\left(|O^{(i)}_{u2}| < |O^{(i)}_{u1}|\Big|O^{(i)}_{u1}\right)\right]. \tag{29}$$

Furthermore, since $\widetilde{H}_{u1}(n)$ and $O^{(i)}_{u1}$ are correlated complex Gaussians, $\left|\widetilde{H}_{u1}(n)\right|$ given $O^{(i)}_{u1}$ can be shown to be a Rician RV with conditional pdf

$$\mathrm{p}_{\left|\widetilde{H}_{u1}(n)\right|\left|O^{(i)}_{u1}\right.}(x) = \frac{2x}{\sigma_i^2}\exp\left(-\frac{x^2+\nu_i^2}{\sigma_i^2}\right) I_0\left(\frac{2x\nu_i}{\sigma_i^2}\right), \quad x \geq 0, \tag{30}$$

where $I_0(\cdot)$ is the modified Bessel function of zeroth order, $\nu_i = \left|\mathbf{E}\left[\widetilde{H}_{u1}(n)\big|O^{(i)}_{u1}\right]\right| = \frac{\left|(\boldsymbol{\Delta}_i(n))_{12}O^{(i)}_{u1}\right|}{(\boldsymbol{\Delta}_i(n))_{22}}$ and $\sigma_i^2 = \mathbf{var}\left[\widetilde{H}_{u1}(n)\big|O^{(i)}_{u1}\right] = \frac{(\boldsymbol{\Delta}_i(n))_{11}(\boldsymbol{\Delta}_i(n))_{22} - \left|(\boldsymbol{\Delta}_i(n))_{12}\right|^2}{(\boldsymbol{\Delta}_i(n))_{22}}$.

Since ν_i is linearly proportional to $|O^{(i)}_{u1}|$, it is a Rayleigh RV with power φ_i^2, which is given by $\varphi_i^2 = \frac{\mathbf{E}\left[(\boldsymbol{\Delta}_i(n))_{12}\left|O^{(i)}_{u1}\right|^2(\boldsymbol{\Delta}_i(n))^\dagger_{12}\right]}{(\boldsymbol{\Delta}_i(n))^2_{22}} = \frac{\left|(\boldsymbol{\Delta}_i(n))_{12}\right|^2}{(\boldsymbol{\Delta}_i(n))_{22}}$. Hence, the second term inside the expectation in (29) is equal to

$$\Pr\left(|O^{(i)}_{u2}| < |O^{(i)}_{u1}|\big|O^{(i)}_{u1}\right) = 1 - \exp\left(-\frac{\nu_i^2}{\varphi_i^2}\right). \tag{31}$$

Combining (28), (29), (30), and (31) into (27), rearranging terms, and using the identities in [35, (6.631.4)], [35, (8.406.1)], and [34, (5A.15)], reduces (27) to the final expression in (14).

C. Proof of Result 2

By symmetry, the probability $P_E^{(1)}(n)$ that a symbol transmitted on the n^{th} subcarrier belonging to the first chunk of PRBs is in error is $P_E^{(1)}(n) = \Pr(\text{Err}|\hat{\phi}_1 = 11)$. Conditioning on the refined estimate and the fact that

$$\mathrm{p}(|\widetilde{H}_{11}(n)| = x|\hat{\phi}_1 = 11) = 2N\mathrm{p}(|\widetilde{H}_{11}(n)| = x, \hat{\phi}_1 = 11),$$

we get

$$P_E^{(1)}(n) = 2N\int_0^\infty \Pr(\text{Err}\big||\widetilde{H}_{11}(n)| = x, \hat{\phi}_1 = 11) \times \mathrm{p}(|\widetilde{H}_{11}(n)| = x, \hat{\phi}_1 = 11)\, dx. \tag{32}$$

Given the refined estimate $\widetilde{H}_{11}(n)$, the decision variable is independent of the SRS channel estimates, and, hence, of the event $\hat{\phi}_1 = 11$. Thus,

$$P_E^{(1)}(n) = 2N\int_0^\infty \Pr(\text{Err}\big||\widetilde{H}_{11}(n)| = x) \times \mathrm{p}(|\widetilde{H}_{11}(n)| = x, \hat{\phi}_1 = 11)\, dx. \tag{33}$$

As in Appendix B, the first term in the integrand above is

$$\Pr(\text{Err}\big||\widetilde{H}_{11}(n)| = x) = \frac{1}{\pi}\int_0^{\frac{(M-1)\pi}{M}} \exp\left(-\frac{L_1 x^2}{\sin^2\theta}\right) d\theta, \tag{34}$$

where L_1 is given in Result 1.

[4]The notation $\mathrm{p}(X = x, A)$, where X is an RV and A is an event, is defined as $\mathrm{p}(X = x, A) = \lim_{\delta\to 0}\frac{\Pr(x \leq X \leq x+\delta, A)}{\delta}$.

Next we evaluate the second term in the integrand in (33). As in Appendix B, let $O_{jk}^{(1)} \triangleq \sum_{p=1}^{C} \widehat{H}_{jk}^{S}(n_p)$, for $j = 1, 2, \cdots, N$ and $k = 1, 2$. Conditioning on $O_{11}^{(1)}$, we get

$$\mathrm{p}(|\widetilde{H}_{11}(n)| = x, \hat{\phi}_1 = 11) = \mathbf{E}\left[\mathrm{p}_{|\widetilde{H}_{11}(n)|\left|O_{11}^{(1)}\right.}(x) \times \Pr\left(\max\{|O_{12}^{(1)}|, \cdots, |O_{N2}^{(1)}|\} < |O_{11}^{(1)}|\middle|O_{11}^{(1)}\right)\right]. \quad (35)$$

Unlike Appendix B, now $(2N-1)$ RVs instead of 1 RV are less than $O_{11}^{(1)}$ due to FDS. $\left|\widetilde{H}_{11}(n)\right|$ given $O_{11}^{(1)}$ can again be shown to be a Rician RV with conditional pdf

$$\mathrm{p}_{|\widetilde{H}_{11}(n)|\left|O_{11}^{(1)}\right.}(x) = \frac{2x}{\sigma_1^2}\exp\left(-\frac{x^2+\nu_{11}^2}{\sigma_1^2}\right) I_0\left(\frac{2x\nu_{11}}{\sigma_1^2}\right), x \geq 0, \quad (36)$$

where $\nu_{11} = \left|\mathbf{E}\left[\widetilde{H}_{11}(n)\middle|O_{11}^{(1)}\right]\right| = \frac{\left|(\boldsymbol{\Delta}_1(n))_{12}O_{11}^{(1)}\right|}{(\boldsymbol{\Delta}_1(n))_{22}}$, and $\sigma_1^2 = \mathbf{var}\left[\widetilde{H}_{11}(n)\middle|O_{11}^{(1)}\right] = (\boldsymbol{\Delta}_1(n))_{11} - \frac{\left|(\boldsymbol{\Delta}_1(n))_{12}\right|^2}{(\boldsymbol{\Delta}_1(n))_{22}}$. Further, ν_{11} is a Rayleigh RV with power $\varphi_1^2 = \frac{\mathbf{E}\left[(\boldsymbol{\Delta}_1(n))_{12}\left|O_{11}^{(1)}\right|^2(\boldsymbol{\Delta}_1(n))_{12}^{\dagger}\right]}{(\boldsymbol{\Delta}_1(n))_{22}^2} = \frac{\left|(\boldsymbol{\Delta}_1(n))_{12}\right|^2}{(\boldsymbol{\Delta}_1(n))_{22}}$.

In (35), conditioning on $O_{11}^{(1)}$ is equivalent to conditioning on ν_{11}. Given $O_{11}^{(1)}$, the RVs $O_{12}^{(1)}, \cdots, O_{N2}^{(1)}$, which occur inside the expectation in (35), are mutually independent. Hence,

$$\begin{aligned}\Pr\left(\max\{|O_{12}^{(1)}|, \cdots, |O_{N2}^{(1)}|\} < |O_{11}^{(1)}|\middle|O_{11}^{(1)}\right) &= \Pr\left(\max\{\nu_{12}, \cdots, \nu_{N2}\} < \nu_{11}\middle|\nu_{11}\right), \\ &= \left(1-\exp\left(-\frac{\nu_{11}^2}{\varphi_1^2}\right)\right)^{2N-1}. \quad (37)\end{aligned}$$

Combining (34), (35), (36), and (37) into (33), rearranging terms, and using the identities in [35, (6.631.4)], [35, (8.406.1)], and [35, (3.312.1)] reduces (33) to (17).

D. Proof of Result 3

By symmetry, the probability $P_E^{(2)}(n)$ that a symbol transmitted on the n^{th} subcarrier belonging to the second chunk of PRBs is in error is $P_E^{(2)}(n) = \Pr(\text{Err}|\hat{\phi}_2 = 21, \hat{\phi}_1 = 11)$. The key point that the analysis below addresses is that the choices of $\hat{\phi}_2$ and $\hat{\phi}_1$ are coupled in (16). Conditioning on the refined estimate, we get

$$P_E^{(2)}(n) = \int_0^{\infty} \Pr(\text{Err}||\widetilde{H}_{21}(n)| = x, \hat{\phi}_2 = 21, \hat{\phi}_1 = 11) \times \mathrm{p}(|\widetilde{H}_{21}(n)| = x|\hat{\phi}_2 = 21, \hat{\phi}_1 = 11)\, dx. \quad (38)$$

Again, given the refined estimate $\widetilde{H}_{21}(n)$, the decision variable is independent of the SRS-based channel estimates, and, hence, the events $\hat{\phi}_1 = 11$ and $\hat{\phi}_2 = 21$. Further, by symmetry,

$$\begin{aligned}&\mathrm{p}(|\widetilde{H}_{21}(n)| = x|\hat{\phi}_2 = 21, \hat{\phi}_1 = 11) \\ &\quad = 4N(N-1)\mathrm{p}(|\widetilde{H}_{21}(n)| = x, \hat{\phi}_2 = 21, \hat{\phi}_1 = 11). \quad (39)\end{aligned}$$

Thus,

$$P_E^{(2)}(n) = 4N(N-1)\int_0^{\infty} \Pr(\text{Err}||\widetilde{H}_{21}(n)| = x) \times \mathrm{p}(|\widetilde{H}_{21}(n)| = x, \hat{\phi}_2 = 21, \hat{\phi}_1 = 11)\, dx. \quad (40)$$

The first term in the integrand in (40) is the same as (34) except that L_1 is replaced by $L_2 = \frac{|\boldsymbol{\Psi}_2(n)\boldsymbol{Q}_2(n)|^2 E_s \sin^2\left(\frac{\pi}{M}\right)}{1+E_s\left(\boldsymbol{\omega}_n\boldsymbol{\Lambda}_h\boldsymbol{\omega}_n^{\dagger} - \boldsymbol{\Psi}_2(n)\boldsymbol{\Delta}_2(n)^{-1}\boldsymbol{\Psi}_2(n)^{\dagger}\right)}$. We now evaluate the second term in the integrand in (40). For the second chunk, let $O_{jk}^{(2)} \triangleq \sum_{p=C+1}^{2C} \widehat{H}_{jk}^{S}(n_p)$, for $j = 2, \cdots, N$ and $k = 1, 2$. Recall that $O_{jk}^{(1)} \triangleq \sum_{p=1}^{C} \widehat{H}_{jk}^{S}(n_p)$, $j = 1, \cdots, N$ and $k = 1, 2$. From the joint AS-FDS algorithm in Sec. IV, we know that

$$\begin{aligned}&\mathrm{p}(|\widetilde{H}_{21}(n)| = x, \hat{\phi}_2 = 21, \hat{\phi}_1 = 11) \\ &\quad = \mathrm{p}(|\widetilde{H}_{21}(n)| = x, \max\{|O_{22}^{(2)}|, \cdots, |O_{N2}^{(2)}|\} < |O_{21}^{(2)}|, \\ &\qquad \max\{|O_{12}^{(1)}|, \cdots, |O_{N2}^{(1)}|\} < |O_{11}^{(1)}|). \quad (41)\end{aligned}$$

Since the channel gains of a user are correlated across subcarriers, the probability of the event $\{\max\{|O_{22}^{(2)}|, \cdots, |O_{N2}^{(2)}|\} < |O_{21}^{(2)}|, \max\{|O_{12}^{(1)}|, \cdots, |O_{N2}^{(1)}|\} < |O_{11}^{(1)}|\}$ is approximately the same as that of the event $\{\max\{|O_{22}^{(2)}|, \cdots, |O_{N2}^{(2)}|\} < |O_{21}^{(2)}|, \max\{|O_{12}^{(2)}|, \cdots, |O_{N2}^{(2)}|\} < |O_{11}^{(2)}|\}$. Furthermore, it can be seen that the latter event is the same as the event $\{\max\{|O_{22}^{(2)}|, \cdots, |O_{N2}^{(2)}|\} < |O_{21}^{(2)}|, \max\{|O_{12}^{(2)}|, |O_{21}^{(2)}|\} < |O_{11}^{(2)}|\}$. Hence,

$$\begin{aligned}&\mathrm{p}(|\widetilde{H}_{21}(n)| = x, \hat{\phi}_2 = 21, \hat{\phi}_1 = 11) \\ &\quad \approx \mathrm{p}(|\widetilde{H}_{21}(n)| = x, \max\{|O_{22}^{(2)}|, \cdots, |O_{N2}^{(2)}|\} < |O_{21}^{(2)}|, \\ &\qquad \max\{|O_{12}^{(2)}|, |O_{21}^{(2)}|\} < |O_{11}^{(2)}|). \quad (42)\end{aligned}$$

As before, $\left|\widetilde{H}_{21}(n)\right|$ given $O_{21}^{(2)}$ is a Rician RV with pdf the same as (36) but with ν_{11} and σ_1^2 replaced by $\nu_{21} = \left|\mathbf{E}\left[\widetilde{H}_{21}(n)\middle|O_{21}^{(2)}\right]\right| = \frac{\left|(\boldsymbol{\Delta}_2(n))_{12}O_{21}^{(2)}\right|}{(\boldsymbol{\Delta}_2(n))_{22}}$ and $\sigma_2^2 = \mathbf{var}\left[\widetilde{H}_{21}(n)\middle|O_{21}^{(2)}\right] = \frac{(\boldsymbol{\Delta}_2(n))_{11}(\boldsymbol{\Delta}_2(n))_{22} - \left|(\boldsymbol{\Delta}_2(n))_{12}\right|^2}{(\boldsymbol{\Delta}_2(n))_{22}}$, respectively.

Further, ν_{21} is a Rayleigh RV with power $\varphi_2^2 = \frac{\mathbf{E}\left[(\boldsymbol{\Delta}_2(n))_{12}\left|O_{21}^{(2)}\right|^2(\boldsymbol{\Delta}_2(n))_{12}^{\dagger}\right]}{(\boldsymbol{\Delta}_2(n))_{22}^2} = \frac{\left|(\boldsymbol{\Delta}_2(n))_{12}\right|^2}{(\boldsymbol{\Delta}_2(n))_{22}}$. Thus, (42) can be written as

$$\begin{aligned}\mathrm{p}(|\widetilde{H}_{21}(n)| = x, \hat{\phi}_2 = 21, \hat{\phi}_1 = 11) &\approx \int_{\nu_{21}=0}^{\infty} \frac{2x}{\sigma_2^2} \times \exp\left(-\frac{x^2+\nu_{21}^2}{\sigma_2^2}\right) I_0\left(\frac{2x\nu_{21}}{\sigma_2^2}\right)\left(1-\exp\left(-\frac{\nu_{21}^2}{\sigma_{\nu_2}^2}\right)\right)^{2N-3} \\ &\quad \times \int_{z=\nu_{21}}^{\infty}\left(1-\exp\left(-\frac{z^2}{\varphi_2^2}\right)\right)\frac{2z}{\varphi_2^2}\exp\left(\frac{-z^2}{\varphi_2^2}\right) \\ &\quad \times \frac{2\nu_{21}}{\varphi_2^2}\exp\left(\frac{-\nu_{21}^2}{\varphi_2^2}\right) dz\, d\nu_{21}. \quad (43)\end{aligned}$$

Substituting (43) in (40) and using the identities in [35, (6.631.4)], [35, (8.406.1)], and [35, (3.312.1)] reduces (40) to (19).

E. Brief Proof of Result 4

For the i^{th} chunk of PRBs, let

$$U_j = \max\left\{\left|\sum_{p=(i-1)C+1}^{iC}\widehat{H}_{j1}^{S}(n_p)\right|, \left|\sum_{p=(i-1)C+1}^{iC}\widehat{H}_{j2}^{S}(n_p)\right|\right\},$$

where $j \in \mathcal{U}$. Let $X_1 = \max\{U_1, \ldots, U_{N-i+1}\}$ and X_2 be the ith largest RV among the N RVs $U_1, \ldots, U_N$.

We first show that $X_1 \geq X_2$, which implies that the SEP when the channel gain is X_1 is lower than that when the channel gain is X_2. This is easy to see because, by definition, X_1 is greater than at least $N-i$ RVs among $U_1, \ldots, U_N$, but X_2 is greater than exactly $N-i$ RVs. Hence, $X_2 \leq X_1$. The SEP expression in (20) then directly follows from Result 2, with number of users equal to $N-i+1$ instead of N.

REFERENCES

[1] S. Sanayei and A. Nosratinia, "Antenna selection in MIMO systems," *IEEE Commun. Mag.*, vol. 42, no. 10, pp. 68–73, Oct. 2004.

[2] A. Ghrayeb and T. M. Duman, "Performance analysis of MIMO systems with antenna selection over quasi-static fading channels," *IEEE Trans. Veh. Technol.*, vol. 52, no. 2, pp. 281–288, Mar. 2003.

[3] Z. Chen, J. Yuan, and B. Vucetic, "Analysis of transmit antenna selection/maximal-ratio combining in Rayleigh fading channels," *IEEE Trans. Veh. Technol.*, vol. 54, no. 4, pp. 1312–1321, July 2005.

[4] W. M. Gifford, M. Z. Win, and M. Chiani, "Diversity with practical channel estimation," *IEEE Trans. Wireless Commun.*, vol. 4, no. 4, pp. 1935–1947, July 2005.

[5] T. Gucluoglu and E. Panayirci, "Performance of transmit and receive antenna selection in the presence of channel estimation errors," *IEEE Commun. Lett.*, vol. 12, no. 5, pp. 371–373, May 2008.

[6] M. Qian and C. Tepedelenlioglu, "Antenna selection for space-time coded systems with imperfect channel estimation," *IEEE Trans. Wireless Commun.*, vol. 6, no. 2, pp. 710–719, Feb. 2007.

[7] N. B. Mehta, A. F. Molisch, and S. Kashyap, "Antenna selection in LTE: from motivation to specification," *IEEE Commun. Mag.*, vol. 50, no. 10, pp. 144–150, Oct. 2012.

[8] N. B. Mehta, A. F. Molisch, J. Zhang, and E. Bala, "Antenna selection training in MIMO-OFDM/OFDMA cellular systems," in *Proc. 2007 CAMSAP*, pp. 113–116.

[9] A. Gorokhov, D. A. Gore, and A. J. Paulraj, "Receive antenna selection for MIMO flat-fading channels: theory and algorithms," *IEEE Trans. Inf. Theory*, vol. 49, no. 10, pp. 2687–2696, Oct. 2003.

[10] A. F. Molisch, M. Z. Win, and J. H. Winters, "Capacity of MIMO systems with antenna selection," in *Proc. 2001 ICC*, pp. 570–574.

[11] ——, "Reduced-complexity transmit/receive-diversity systems," *IEEE Trans. Signal Process.*, vol. 51, no. 11, pp. 2729–2738, Nov. 2003.

[12] M. Torabi and D. Haccoun, "Performance analysis of joint user scheduling and antenna selection over MIMO fading channels," *IEEE Signal Process. Lett.*, vol. 18, no. 4, pp. 235–238, Apr. 2011.

[13] C.-J. Chen and L.-C. Wang, "A unified capacity analysis for wireless systems with joint multiuser scheduling and antenna diversity in Nakagami fading channels," *IEEE Trans. Commun.*, vol. 54, no. 3, pp. 469–478, Mar. 2006.

[14] X. Zhang, F. Chen, and W. Wang, "Outage probability study of multiuser diversity in MIMO transmit antenna selection systems," *IEEE Signal Process. Lett.*, vol. 14, no. 3, pp. 161–164, Mar. 2007.

[15] V. Kristem, N. B. Mehta, and A. F. Molisch, "Optimal receive antenna selection in time-varying fading channels with practical training constraints," *IEEE Trans. Commun.*, vol. 58, no. 7, pp. 2023–2034, July 2010.

[16] M. Torabi, "Antenna selection for MIMO-OFDM systems," *Signal Process.*, vol. 88, no. 10, pp. 2431–2441, Oct. 2008.

[17] M. Torabi, D. Haccoun, and W. Ajib, "Performance analysis of scheduling schemes for rate-adaptive MIMO OSFBC-OFDM systems," *IEEE Trans. Veh. Technol.*, vol. 59, no. 5, pp. 2363–2379, June 2010.

[18] A. Wilzeck and T. Kaiser, "Antenna subset selection for cyclic prefix assisted MIMO wireless communications over frequency selective channels," *EURASIP J. Adv. Signal Process*, vol. 130, pp. 1–14, Jan. 2008.

[19] I. Bahceci, T. M. Duman, and Y. Altunbasak, "Performance of MIMO antenna selection for space-time coded OFDM systems," in *Proc. 2004 WCNC*, pp. 987–992.

[20] H. Zhang and R. U. Nabar, "Transmit antenna selection in MIMO-OFDM systems: Bulk versus per-tone selection," in *Proc. 2008 ICC*, pp. 4371–4375.

[21] M. Sandell and J. Coon, "Performance of combined bulk and per-tone antenna selection precoding in coded OFDM systems," *IEEE Trans. Commun.*, vol. 60, no. 3, pp. 655–660, Mar. 2012.

[22] A. B. Narasimhamurthy and C. Tepedelenlioglu, "Antenna selection for MIMO-OFDM systems with channel estimation error," *IEEE Trans. Veh. Technol.*, vol. 58, no. 5, pp. 2269–2278, June 2009.

[23] Mitsubishi Electric and NTT DoCoMo, "Low cost training for transmit antenna selection on the uplink," Tech. Rep. R1-062941, 3GPP RAN1#46bis, Oct. 2006.

[24] S. Guharoy and N. B. Mehta, "Joint evaluation of channel feedback schemes, rate adaptation, and scheduling in OFDMA downlinks with feedback delays," *IEEE Trans. Veh. Technol.*, vol. 62, no. 4, pp. 1719–1731, May 2013.

[25] Y.-J. Choi and S. Bahk, "Partial channel feedback schemes maximizing overall efficiency in wireless networks," *IEEE Trans. Wireless Commun.*, vol. 7, no. 4, pp. 1306–1314, Apr. 2008.

[26] M. Z. Win and J. H. Winters, "Analysis of hybrid selection/maximal-ratio combining in Rayleigh fading," *IEEE Trans. Commun.*, vol. 47, no. 12, pp. 1773–1776, Dec. 1999.

[27] M.-S. Alouini and M. K. Simon, "Application of the Dirichlet transformation to the performance evaluation of generalized selection combining over Nakagami-m fading channels," *J. Commun. Netw.*, vol. 1, pp. 5–13, 1999.

[28] ——, "Performance of coherent receivers with hybrid SC/MRC over Nakagami-m fading channels," *IEEE Trans. Veh. Technol.*, vol. 48, no. 4, pp. 1155–1164, July 1999.

[29] L. de Temino, G. Berardinelli, S. Frattasi, K. Pajukoski, and P. Mogensen, "Single-user MIMO for LTE-A uplink: performance evaluation of OFDMA vs. SC-FDMA," in *Proc. 2009 Radio Wireless Symp.*, pp. 304–307.

[30] J. P. Coon and M. Sandell, "Combined bulk and per-tone transmit antenna selection in OFDM systems," *IEEE Commun. Lett.*, vol. 14, no. 5, pp. 426–428, May 2010.

[31] S. Sesia, I. Toufik, and M. Baker, *LTE – The UMTS Long Term Evolution, From Theory to Practice*. John Wiley and Sons, 2009.

[32] S. M. Kay, *Fundamentals of Statistical Signal Processing: Estimation Theory*, 1st ed. Prentice Hall Signal Processing Series, 1993, vol. 1.

[33] "Deployment aspects," 3rd Generation Partnership Project (3GPP), Tech. Rep. 25.943 v6.0.0 (2004-12).

[34] M. Simon and M.-S. Alouini, *Digital Communication over Fading Channels*, 2nd ed. Wiley-Interscience, 2005.

[35] I. S. Gradshteyn and I. M. Ryzhik, *Tables of Integrals, Series and Products*. Academic Press, 2000.

Salil Kashyap received his Bachelor of Technology degree in Electronics and Communication Eng. from NERIST, Itanagar in 2007 and Master of Technology degree in Digital Signal Processing from the Indian Institute of Technology (IIT), Guwahati in 2009. He is currently working towards his Ph.D. in the Dept. of Electrical Communication Eng., at the Indian Institute of Science (IISc), Bangalore. His research interests include cognitive radio and performance analysis of antenna selection and resource allocation algorithms in MIMO-OFDMA systems.

Neelesh B. Mehta (S'98-M'01-SM'06) received his Bachelor of Technology degree in Electronics and Communications Eng. from the Indian Institute of Technology (IIT), Madras in 1996, and his M.S. and Ph.D. degrees in Electrical Eng. from the California Institute of Technology, Pasadena, USA in 1997 and 2001, respectively. He is now an Associate Professor in the Dept. of Electrical Communication Eng., Indian Institute of Science (IISc), Bangalore. He serves an Editor for IEEE WIRELESS COMMUNICATIONS LETTERS and as the Director of Conference Publications on the Board of Governors of IEEE Comsoc.